

# Pressure-induced metal-insulator and spin-state transition in low-valence layered nickelates

Victor Pardo\* and Warren E. Pickett†

*Department of Physics, University of California, Davis, California 95616, USA*

(Received 22 June 2011; revised manuscript received 28 November 2011; published 12 January 2012)

*Ab initio* calculations predict a metal-insulator transition at zero temperature to occur in  $\text{La}_4\text{Ni}_3\text{O}_8$  at moderate pressures as a result of a pressure-induced spin-state transition. The spin-state transition that is seen at 105 K at ambient pressure, from a low-temperature high-spin state to a high-temperature low-spin state, has been observed to be shifted to lower temperatures as pressure is applied. From our calculations, we find that a smaller unit cell volume favors the metallic low-spin state, which becomes more stable at 5 GPa. Similar physics appears in the related compound  $\text{La}_3\text{Ni}_2\text{O}_6$ , but on a different energy scale, which may account for why the transition has not been observed in this material.

DOI: [10.1103/PhysRevB.85.045111](https://doi.org/10.1103/PhysRevB.85.045111)

PACS number(s): 71.20.-b, 71.30.+h, 75.47.Lx

## I. INTRODUCTION

Spin-state transitions are observed in a variety of multi-orbital systems as a result of the competition between Hund's rule coupling  $J_H$  and crystal-field strength  $\Delta_{cf}$  that separates orbitals in energy. Typical examples are  $\text{LaCoO}_3$ , where  $\text{Co}^{3+}:d^6$  cations in an octahedral environment can occur in a nonmagnetic low-spin (LS) state and various excited magnetic spin states [both intermediate spin (IS) and high spin (HS) have been predicted<sup>1</sup>] due to  $J_H$  of the cation being the same order of magnitude as  $\Delta_{cf}$ . Various Fe compounds also show spin-state transitions, and this is a common feature in organometallics literature,<sup>2</sup> where metal cations can be tuned to be in different spin states. It is common that the LS state is more stable at lower temperatures, although in some systems the opposite occurs.<sup>3</sup> Important competition between  $\Delta_{cf}$  and  $J_H$  at high pressure has also been found in the calculation of the Mott transition in  $\text{MnO}$  by Kuneš *et al.*,<sup>4</sup> where the insulator-metal transition, moment collapse (high spin to low spin), and volume collapse are found (experimentally and theoretically) just above 100 GPa. The pressure at which the transition occurs is sensitive to competition between these two energy scales, and not to the interaction strength  $U$  to bandwidth  $W$  ratio.<sup>4</sup>

$\text{La}_4\text{Ni}_3\text{O}_8$  (La438) and  $\text{La}_3\text{Ni}_2\text{O}_6$  (La326), synthesized and characterized recently by Greenblatt's group,<sup>5-9</sup> are ionic but highly unconventional insulators. As the  $n = 3$  and  $n = 2$  members, respectively, of the sequence of compounds  $\text{La}_{n+1}\text{Ni}_n\text{O}_{2n+2}$ , they have a Ni formal valence  $(n+1)/n$  which, being noninteger, corresponds to metallic intermediate valent behavior, yet both are insulating. The structure (space group  $I4/mmm$ , no. 139) consists of  $n$  "infinite layer"  $\text{NiO}_2$  square nets separated by La ions, and these  $n$ -layer slabs are separated by fluorite structure La-O<sub>2</sub>-La blocking (and charge-contributing) layers. Structurally, the formula can be pictured as  $(\text{La}_2\text{O}_2)(\text{NiO}_2)_n\text{La}_{n-1}$ . For the  $n = 3$  case, it might be expected that charge ordering  $\text{Ni}^{2+} + 2\text{Ni}^+$  would arise (note there is one inner Ni layer and two outer Ni layers). However, attempts to produce such an insulating state in electronic structure calculations were not successful,<sup>5,10</sup> and the insulating character of La438 was shown to be understood only in terms of Mott insulating  $\text{Ni}_3$  molecular orbitals<sup>10</sup> (rather than atomic orbitals).

As a low-valence nickelate, La438 has drawn attention<sup>5</sup> because of similarities in its crystallographic and electronic

structure to superconducting cuprates. The blocking  $\text{La}_2\text{O}_2$  layer effectively isolates successive nickelate slabs electronically,<sup>10</sup> providing a highly two-dimensional electronic structure. Two different Ni sites exist in the structure, in the inner and outer layers of the  $\text{NiO}_2$  trilayers. The compound undergoes a phase transition at 105 K that, based on  $^{139}\text{La}$  nuclear-magnetic-resonance measurements, has been described as a transition to an unconventional low-temperature antiferromagnetic (AF) phase.<sup>11</sup> Their data for  $1/T_1T$  vs  $T$  ( $T_1$  is the spin-lattice relaxation time) contain a constant contribution above the transition as in metals, and was interpreted as arising from spin scattering with quasiparticles at the Fermi surface. However, above the transition the resistivity remains high with an insulatorlike increase as temperature is lowered. The low-temperature data, both the resistivity and the heat capacity, indicate a highly insulating ground state. Recent structural studies by Lokshin and Egami<sup>12</sup> suggest the transition involves a spin-state transition on the Ni cations.

Focusing on an atomic (rather than molecular) picture, two possible spin states can occur in La438. The (on average)  $\text{Ni}^{1.33+}:d^{8.67}$  cations sit in a square planar environment that leads to a large splitting  $\Delta_{cf}$  between the  $d_{x^2-y^2}$  and  $d_{z^2}$  bands, a result of the absence of apical oxygens in this low-valence nickelate. Within the  $e_g$  doublet,  $\Delta_{cf}$  can become comparable to  $J_H$ ; if the former is larger, a LS state develops, but if  $J_H$  dominates, larger moments and therefore the HS state will be more stable. This distinction is depicted in Fig. 1. This simple picture of the electronic structure of the compound suggests that the HS state would have a larger in-plane lattice parameter due to the somewhat greater occupation of the  $d_{x^2-y^2}$  orbital, as well as a smaller Ni-Ni interplane distance due to the deoccupation of the  $d_{z^2}$  antibonding orbital, consistent with measurements.<sup>12</sup> In addition, the HS state leads to an in-plane AF coupling being more stable,<sup>10</sup> consistent with the observation of magnetic order below 105 K.

As can be foreseen from Fig. 1, the HS and LS states will lead to quite different properties. The HS ion provides an insulating state arising from the formation of Mott insulating  $d_{z^2}$  molecular orbitals.<sup>10</sup> These molecular orbitals are bonding-antibonding split around the Fermi level due to their strong  $\sigma$  bond along the  $c$  axis (relative to their intraplanar hopping). On the other hand, the LS state is characterized by a  $2/3$ -filled  $d_{x^2-y^2}$ , metallic band at the Fermi level. The observed

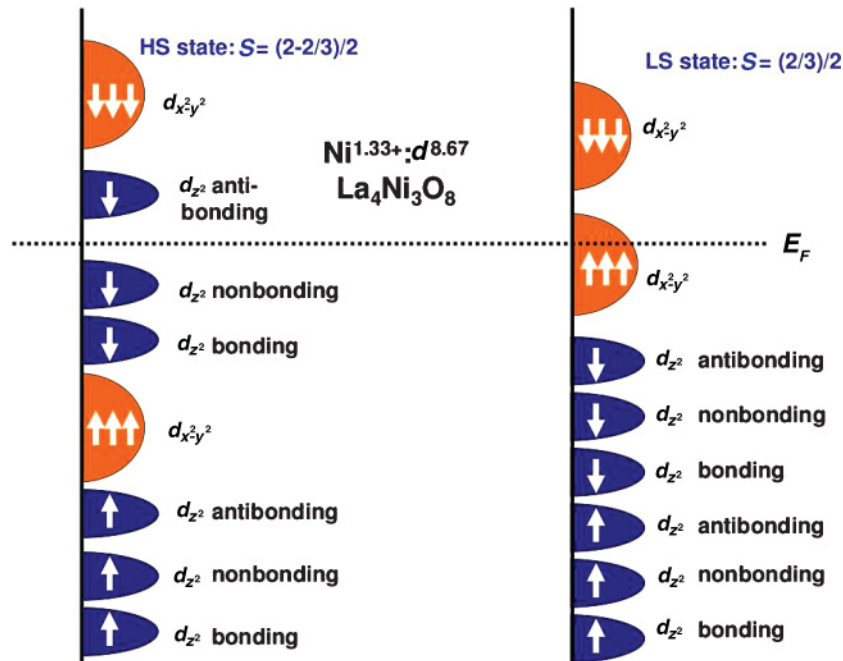


FIG. 1. (Color online) Two possible spin states in the trilayer Ni compound La438 are presented schematically, distinguished by the strength of the crystal-field splitting between the  $d_{z^2}$  and  $d_{x^2-y^2}$  orbitals and the Hund’s rule coupling strength. The  $d_{z^2}$  and  $d_{x^2-y^2}$  are distinguished by color for clarity. On the left side, the high-spin state (larger Hund’s rule coupling) is pictured, with the contrasting low-spin state on the right (corresponding to larger crystal-field splitting). Three Ni atoms are represented to account for the strong coupling along the  $c$  axis and the formation of molecular orbitals with  $d_{z^2}$  parentage. The Fermi level  $E_F$  is denoted by the horizontal line, lying in the insulating HS gap, but cutting through metallic LS bands.

reduction in resistivity<sup>5</sup> above the phase transition at 105 K (though still insulating) is consistent with at least an admixture of some Ni atoms in a LS state above the transition. If all Ni atoms assume a LS configuration, the system becomes metallic.

La438 and La326 are compounds close to a metal-insulator transition, one that can be driven metallic by oxygen doping while maintaining the underlying structure.<sup>13</sup> This transition has been studied recently for the  $\text{La}_3\text{Ni}_2\text{O}_{7-\delta}$  series.<sup>14</sup> Both high- and low-spin states are obtained in density-functional-based calculations having similar energies. It will be shown below that this quasidegeneracy makes this system a good probe of the mechanism that underlies the unusual behavior observed in this class of nickelates.

In this paper, we use the low-valence compounds La326 and La438 to explore the evolution of both spin states, and their relative stability, with respect to different physical and computational variables: volume compression corresponding to applied pressure, the magnitude of Coulomb repulsion  $U$  in the Ni  $3d$  shell, and the choice of LDA +  $U$  functional (which one is most applicable is not obvious). The results suggest that a spin-state transition can be achieved at moderate pressure, and can be readily monitored by the corresponding reduction in resistivity because it is also an insulator-metal transition, unlike the magnetic ordering transition at 105 K.

## II. COMPUTATIONAL PROCEDURES

Electronic structure calculations were performed within density-functional theory<sup>15,16</sup> using the all-electron, full potential code WIEN2K<sup>17</sup> based on the augmented plane wave plus local orbital (APW + lo) basis set.<sup>18</sup> The generalized gradient approximation<sup>19</sup> (GGA) was used for the structure optimizations at each volume (that include both optimizations of the  $c/a$  ratio and the atomic positions) to determine the equation of state of the system. Pressure values were obtained by fitting energy versus volume data to the Murnaghan<sup>20</sup> and,

for a consistency check, also the Birch-Murnaghan<sup>21</sup> equations of state.

To deal with strong correlation effects that are widely acknowledged to play an important role in nickelates, we apply the LDA +  $U$  scheme<sup>22,23</sup> that incorporates an on-site repulsion  $U$  and  $J_H$  for the Ni  $3d$  states. For the uncorrelated part of the exchange-correlation functional, we used the local density approximation (LDA),<sup>24</sup> except for the structural relaxations mentioned above. Results presented below compare two widely used LDA +  $U$  schemes: the so-called “fully localized limit”<sup>25</sup> (FLL) and the “around the mean field”(AMF) scheme.<sup>26</sup> A description of the results obtained at different values of  $U$  (in a reasonably broad range 4.5–8.5 eV for the Ni cations) is given in the main text below. The value chosen for the on-site Hund’s rule strength is  $J = 0.68$  eV and is kept fixed. All calculations were converged with respect to all the parameters to beyond the precision required for the results that we quote. Specifically, we used  $R_{\text{mt}}K_{\text{max}} = 6.0$ , a  $k$ -mesh of  $10 \times 10 \times 2$ , and muffin-tin radii of 2.35 a.u. for La, 1.97 a.u. for Ni, and 1.75 a.u. for O.

## III. RESULTS

### A. $\text{La}_4\text{Ni}_3\text{O}_8$

For this compound, the electronic structure of the Mott insulating HS state has been described extensively elsewhere.<sup>10,14</sup> Here we focus on the electronic and magnetic structure of the LS state. Band dispersion along  $k_z$  is negligible in this highly two-dimensional layered structure, so only the two-dimension Brillouin zone needs to be considered. This state, in agreement with a previous report,<sup>5</sup> has in-plane ferromagnetic (FM) coupling due to the less than half-filled  $d_{x^2-y^2}$  in-plane orbital, and the interplanar coupling is AF and weak. The band structure is shown in Fig. 2, with the “fat bands” highlighting the  $e_g$  orbitals of the outer Ni atoms. The electronic structure in this phase was pictured schematically in the right panel of

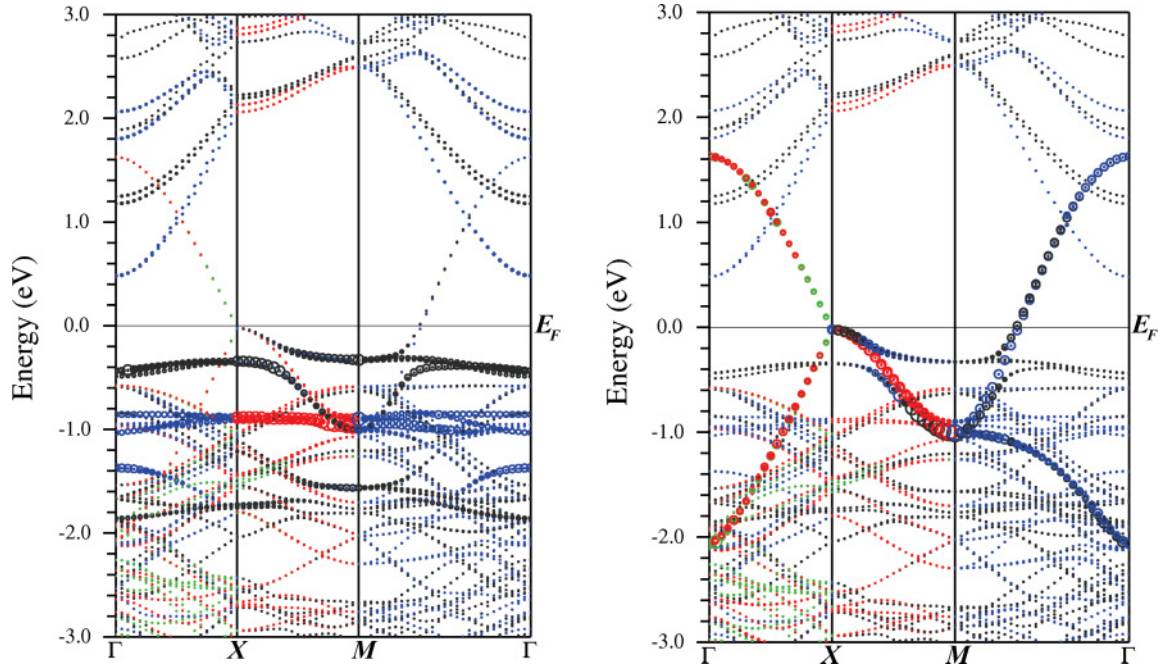


FIG. 2. (Color online) LDA +  $U$  band structure (AMF,  $U = 6.8$  eV) of the LS state of La438. On the left (right) panel, the  $d_{z^2}$  ( $d_{x^2-y^2}$ ) bands are highlighted. The  $2/3$ -filled  $d_{x^2-y^2}$  crosses the Fermi level, leading to a metallic result. The color is only to help distinguish bands.

Fig. 1, with  $d_{z^2}$  bands fully occupied. The left panel of Fig. 2 shows the minority-spin Ni  $d_{z^2}$  bands highlighted; they are split into the bonding, nonbonding, and antibonding bands, all occupied. As described in Ref. 10, the inner Ni atoms do not contribute to the nonbonding  $d_{z^2}$  molecular state.

The partly filled  $d_{x^2-y^2}$  bands, with a bandwidth of 3.5 eV, cross the Fermi level giving a metal. These states are essentially degenerate for both outer and inner Ni atoms, so all layers will conduct. In the band structure of the HS state (see Refs. 10 and 14), the  $d_{x^2-y^2}$  bands are narrower, their bandwidth being reduced substantially by the AF in-plane coupling. AF coupling is not stable in the case of a LS state due to the different (partial) filling of the  $d_{x^2-y^2}$  band.

Comparison of the energy differences of the two possible spin states is presented in Fig. 3, where the energy difference is plotted versus  $U$  (in a reasonable range of 4.5 to 8.5 eV), and for the two LDA +  $U$  schemes (FLL and AMF). When two spin states are nearly degenerate, as here, it is unclear which functional is most appropriate. FLL predicts the HS state to be more stable for all values of  $U$ , with its stability increasing as  $U$  is increased. The AMF scheme is known to favor the stabilization of LS states,<sup>23</sup> and this trend is observed in Fig. 3. With the AMF method, the spin states are degenerate at  $U = 6.5$  eV, with the HS (LS) state being favored at larger (smaller) values of  $U$ . For both functionals, larger  $U$  favors the HS state.

The relative energetics of the different spin states in La438 are therefore uncertain at the *ab initio* level, but we can make inferences from experiment. A magnetic ordering transition to the HS state below 105 K is observed.<sup>12</sup> Supposing that at temperatures above the transition the LS state can be thermally accessed (contributing and perhaps causing the disorder above 105 K), we infer that the energy difference between spin states is  $\sim 100$  K ( $\sim 10$  meV/Ni). This (very small) difference in

Fig. 3 is what is given by the AMF scheme with a  $U \approx 6.6$ – $6.8$  eV. For this reason, we have used AMF and this value of  $U$  for the band structures presented in Fig. 2.

### B. Pressure dependence

A motivation for this work was to study which spin state becomes favored under pressure. To do this, we utilize the AMF scheme with  $U = 6.8$  eV, as determined above to be most realistic. We know of no guideline *a priori* for which spin state will be favored under pressure, when there are so many energy

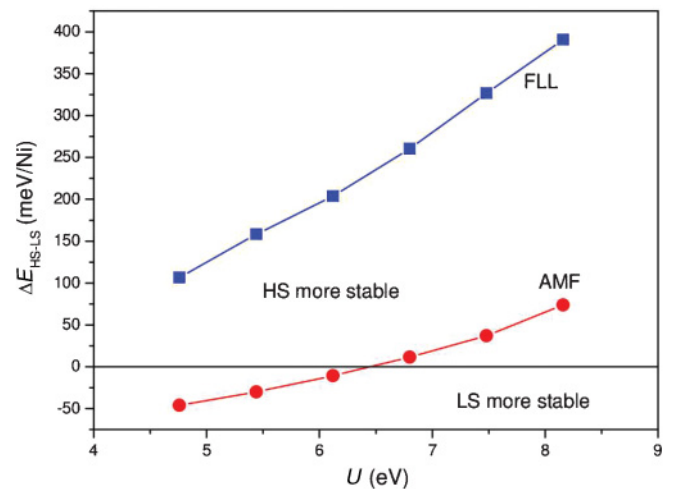


FIG. 3. (Color online) Evolution of the total energy difference between the HS and the LS states with variation of  $U$ , for the two types of LDA +  $U$  schemes we have used: FLL (fully localized limit) and AMF (around the mean field). Positive (negative) energy differences indicate the HS (LS) state is more stable. A crossover is found for the AMF scheme at  $U = 6.5$  eV.

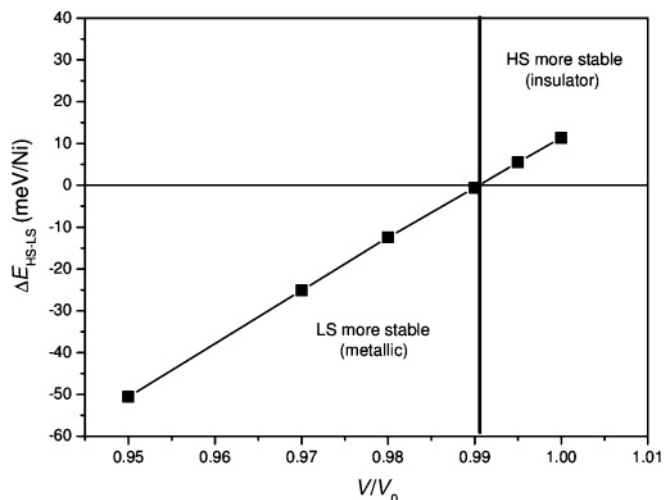


FIG. 4. Evolution of the total energy difference between the HS and the LS states vs volume. The LS state becomes more stable as pressure is applied (at lower volumes). Calculations were carried out with the AMF LDA +  $U$  scheme for  $U = 6.8$  eV (see text). Given the calculated bulk modulus  $B = 180$  GPa (see text), the figure shows a region of  $\Delta P = B|\Delta V/V|$  of 9 GPa.

scales in the system. The energies coming into play will be the relative position of the two  $e_g$  states ( $\Delta_{cf}$ ) and the bonding-antibonding splitting in the  $d_{z^2}$  bands, Hund’s coupling  $J_H$ , but also the general feature of band broadening when volume is reduced. Applying pressure (decreasing the volume) reduces the Ni-Ni interplanar distance, which enhances the bonding-antibonding splitting (a primary effect of which is promoting a HS state).

However, the decrease in volume with pressure also lowers the relative energy of the  $d_{z^2}$  band (a stronger metal-metal bond along the  $c$  axis produces a larger  $d_{z^2}$  occupation to screen the repulsion). Reduction of the Ni-Ni distance within the layer destabilizes the  $d_{x^2-y^2}$  occupation, favoring the LS state. All in all, several energies need to be taken into account self-consistently, which can only be done by carrying out the calculations.

To make a precise determination of the equation of state (hence the bulk modulus relating volume to pressure), we carried out a series of GGA calculations including structural optimization at each volume. GGA is known to give good estimates of lattice constants and internal coordinates, and this is generally not improved by the LDA +  $U$  method. The calculated lattice parameters are  $a = 3.95$  Å,  $c = 26.42$  Å, in good agreement with the experimental<sup>5</sup>  $a = 3.96$  Å,  $c = 26.04$  Å, and result in a unit cell volume 1.5% larger than the observed value. The fit to the equation of state gives a bulk modulus  $B = 180$  GPa (and pressure derivative of  $B$  in the range 25–30, depending on the equation of state used).

The volume dependence of the energy difference, shown in Fig. 4, is 17 meV/% volume change or about 10 meV/GPa change with pressure. It is evident that a reduction in volume favors the LS state. On the scales of energies we are considering, this change in the energy difference is very rapid. Presuming as above that the 105 K transition temperature provides a rough scale of energy difference between spin states, we estimate that the spin-state, insulator-to-metal transition from HS to LS at zero temperature will occur at the modest pressure of 5 GPa or less. Since the LS state is metallic, the transition is detectable by resistivity measurements under pressure.

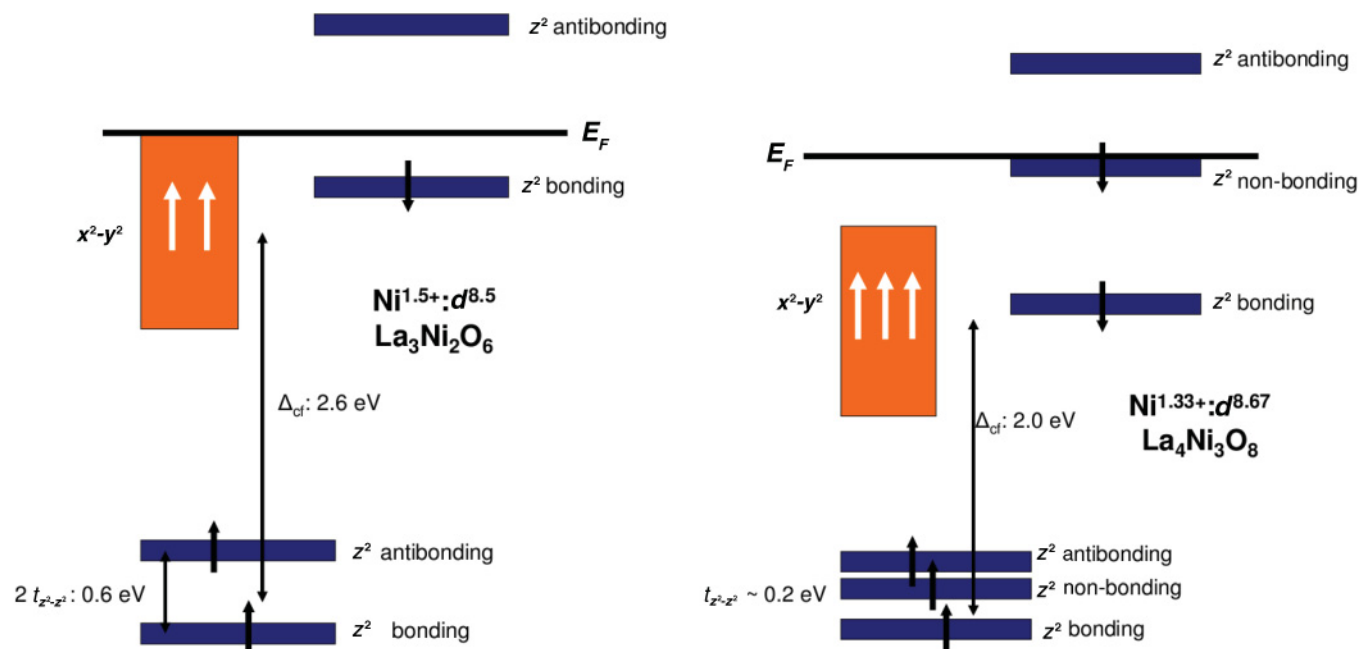


FIG. 5. (Color online) Quantitative comparison of band positions and widths, obtained for La438 and La326 in Refs. 10 and 14 from LDA +  $U$  calculations. Observe that a smaller crystal-field splitting and a larger bonding-antibonding splitting occur for La326 compared to La438. Three (two) Ni atoms are represented for the case of La438 (La326) to account for the bonding-antibonding splitting of the  $d_{z^2}$  bands. Color is used to make the distinction between the crystal-field partner states clearer.

### C. Comparison with $\text{La}_3\text{Ni}_2\text{O}_6$

Generally viewed, the physics of the spin-state transition is quite similar in La326 to that in La438. However, at ambient pressure, the former does not show experimentally any signature of a spin-state transition<sup>8</sup> in susceptibility, resistivity, or heat capacity. The picture that emerges indicates the same metal-insulator transition should occur, although on different energy (therefore pressure and temperature) scales. The lack of experimental input about the energetics of the two possible spin states prevents us from being able to estimate the pressure required for the transition. (Recall that for La438 we used the observed transition temperature together with our energy differences.)

The band structures presented in Refs. 10 and 14, using the same value of  $U$  and the same LDA +  $U$  scheme (FLL) for the HS state, can be used to extract the determining electronic energies  $t_{d_{2^2}-d_{z^2}}$ , the hopping amplitude for the  $\sigma$  bond between Ni cations along the  $c$  axis, and  $\Delta_{\text{cf}}$ , the intra- $e_g$  crystal-field splitting). These values are presented in Fig. 5 along the band center position. In La326,

$$t_{d_{2^2}-d_{z^2}} = 0.3 \text{ eV}, \quad \Delta_{\text{cf}} = 2.6 \text{ eV}, \quad (1)$$

while, for La438,

$$t_{d_{2^2}-d_{z^2}} = 0.2 \text{ eV}, \quad \Delta_{\text{cf}} = 2.0 \text{ eV}. \quad (2)$$

These differences are consistent with the structural differences: the Ni-Ni interlayer distance of 3.96 Å is the same, while La438 has a larger out-of-plane Ni-Ni separation (3.25 vs 3.19 Å). The larger crystal-field splitting in La326 favors the LS state with respect to La438, while the larger bonding-antibonding splitting in La326 tends to favor the HS state. Thus, while similar physical properties are expected in these compounds because the mechanisms are so similar, the uncertainty in the energetics translates to uncertain predictions purely *ab initio*. One difference that may be important is the nonbonding  $d_{z^2}$  band in La438 (due to the third Ni layer) that lies just 0.3 eV above the top of the occupied  $d_{x^2-y^2}$  band (see right panel of Fig. 5).

To gain more information on the energetics governing a spin-state transition in La326, we computed the energy difference between the HS and LS states for both LDA +  $U$  schemes and the same range of  $U$  values as we did for La438, also using the experimental structure.<sup>9</sup> The slightly smaller  $d$  occupation (nominally  $d^{8.5}$  vs  $d^{8.67}$  in La438) suggests some differences, but most likely small ones. The results, shown in Fig. 6, show clear differences with those of La438 shown in Fig. 3. FLL favors the HS state, and AMF the LS state, over the entire range of  $U$ .

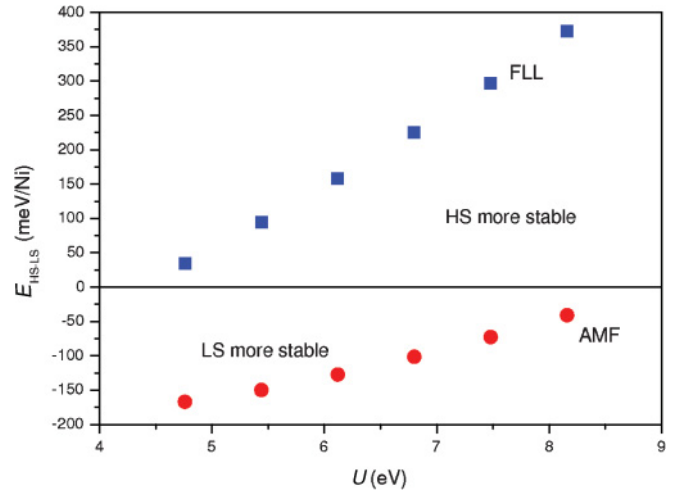


FIG. 6. (Color online) Evolution of the total energy difference of La326 between HS and LS states vs  $U$ , for the two LDA +  $U$  schemes (FLL and AMF), analogous to Fig. 3. Positive (negative) energy differences indicate the HS (LS) state is more stable. See the text for a comparison with La438.

### IV. SUMMARY

*Ab initio* calculations for the compound La438 are applied to obtain the energetics of the spin-state transition that has been expected for this type of compound. A low-temperature HS state, observed experimentally, is found to be the ground state in our calculations at ambient pressure. The evolution of the energy differences and the electronic structure with pressure indicate the metallic LS state will become stable at moderate pressure ( $\sim 5$  GPa). This spin-state transition is accompanied by an insulator-metal transition that may be more easily observable in pressure experiments. This same approach to the energetics and the electronic structure also indicates a similar transition in La326 where, unlike in La438, no data on the transition is yet available. The electronic structure parameters that result from our analysis agree qualitatively with the difference in lattice constants of the two compounds.

### ACKNOWLEDGMENTS

This work grew from questions posed by D. I. Khomskii about which spin state becomes favored at high pressure. The authors acknowledge the exchange of results in the same family of compounds with K. A. Lokshin, J. W. Freeland, C. H. Yee, and G. Kotliar, most of them prior to their publication. This project was supported by Department of Energy Grant No. DE-FG02-04ER46111.

\*victor.pardo@usc.es

†wepickett@ucdavis.edu

<sup>1</sup>M. A. Seánrís-Rodríguez and J. B. Goodenough, *J. Solid State Chem.* **116**, 224 (1995).

<sup>2</sup>P. Gütllich, Y. García, and H. A. Goodwin, *Chem. Soc. Rev.* **29**, 419 (2000).

<sup>3</sup>V. L. Moruzzi, *Phys. Rev. B* **41**, 6939 (1990).

<sup>4</sup>J. Kuneš, A. V. Lukoyanov, V. I. Anisimov, R. T. Scalettar, and W. E. Pickett, *Nat. Mater.* **7**, 198 (2008).

<sup>5</sup>V. V. Poltavets, K. A. Lokshin, A. H. Nevidomskyy, M. Croft, T. A. Tyson, J. Hadermann, G. V. Tendeloo, T. Egami, G. Kotliar, N. ApRoberts-Warren, A. P. Diogardi, N. J. Curro, and M. Greenblatt, *Phys. Rev. Lett.* **104**, 206403 (2010).

<sup>6</sup>V. V. Poltavets, K. A. Lokshin, T. Egami, and M. Greenblatt, *Mater. Res. Bull.* **41**, 955 (2006).

<sup>7</sup>Z. Zhang and M. Greenblatt, *J. Solid State Chem.* **117**, 236 (1995).

- <sup>8</sup>V. V. Poltavets, M. Greenblatt, G. H. Fecher, and C. Felser, *Phys. Rev. Lett.* **102**, 046405 (2009).
- <sup>9</sup>V. V. Poltavets, K. A. Loshin, S. Dikmen, M. Croft, T. Egami, and M. Greenblatt, *J. Am. Chem. Soc.* **128**, 9050 (2006).
- <sup>10</sup>V. Pardo and W. E. Pickett, *Phys. Rev. Lett.* **105**, 266402 (2010).
- <sup>11</sup>N. Ap Roberts-Warren, A. P. Dioguardi, V. V. Poltavets, M. Greenblatt, P. Klavins, and N. J. Curro, *Phys. Rev. B* **83**, 014402 (2011).
- <sup>12</sup>K. Lokshin and T. Egami, [<http://meetings.aps.org/Meeting/MAR11/Event/141968>].
- <sup>13</sup>Y. Kobayashi, S. Taniguchi, M. Kasai, M. Sato, T. Nishioka, and M. Kontani, *J. Phys. Soc. Jpn.* **65**, 3978 (1996).
- <sup>14</sup>V. Pardo and W. E. Pickett, *Phys. Rev. B* **83**, 245128 (2011).
- <sup>15</sup>P. Hohenberg and W. Kohn, *Phys. Rev.* **136**, B864 (1964).
- <sup>16</sup>R. O. Jones and O. Gunnarsson, *Rev. Mod. Phys.* **61**, 689 (1989).
- <sup>17</sup>K. Schwarz and P. Blaha, *Comput. Mater. Sci.* **28**, 259 (2003).
- <sup>18</sup>E. Sjöstedt, L. Nördstrom, and D. J. Singh, *Solid State Commun.* **114**, 15 (2000).
- <sup>19</sup>J. P. Perdew, K. Burke, and M. Ernzerhof, *Phys. Rev. Lett.* **77**, 3865 (1996).
- <sup>20</sup>F. D. Murnaghan, *Proc. Natl. Acad. Sci. USA* **30**, 244 (1944).
- <sup>21</sup>F. Birch, *Phys. Rev.* **71**, 809 (1947).
- <sup>22</sup>V. I. Anisimov, J. Zaanen, and O. K. Andersen, *Phys. Rev. B* **44**, 943 (1991).
- <sup>23</sup>E. R. Ylvisaker, W. E. Pickett, and K. Koepf, *Phys. Rev. B* **79**, 035103 (2009).
- <sup>24</sup>J. P. Perdew and Y. Wang, *Phys. Rev. B* **45**, 13244 (1992).
- <sup>25</sup>A. G. Petukhov, I. I. Mazin, L. Chioncel, and A. I. Lichtenstein, *Phys. Rev. B* **67**, 153106 (2003).
- <sup>26</sup>M. T. Czyzyk and G. A. Sawatzky, *Phys. Rev. B* **49**, 14211 (1994).